Rheol Acta (2011) 50:955–964
DOI 10.1007/s00397-011-0581-y

ORIGINAL CONTRIBUTION

Dispersion of multi-walled carbon nanotubes in PDMS/PB blend

Joung Sook Hong · Chongyoup Kim

Received: 8 June 2010 / Revised: 17 November 2010 / Accepted: 20 January 2011 / Published online: 19 August 2011

Abstract In this study, the sequential dispersion of multi-walled carbon nanotubes (CNTs) in PDMS/PB (polydimethylsiloxane/polybutene) blends and the change of blend morphology by the dispersion of CNTs were investigated by rheological and morphological observations. The dispersion of CNTs into PDMS/PB blend was accomplished by the dilution of the CNT master (2 wt.% CNT in PDMS) in PDMS/PB blend using an extensional mixer. The morphological study shows that under the extensional flow, CNTs in the dispersed CNT master phase are mainly broken up by tip-streaming and the continuous pinching-off of PDMS drops during morphology evolution enhances the dispersion of CNT. It has been shown that CNTs can be disentangled as in the case of dispersing CNTs in a Boger fluid. Rheological data and TEM observations show that it is not simply a mixing of two phases and the CNTs in the master phase can be dispersed in the single CNT level.

Keywords Extensional flow · Pinch-off mechanism · CNT disentanglement

This paper was presented at the 6th Annual European Rheology Conference, April 7–9, 2010 in Göteborg, Sweden.

J. S. Hong
Department of Chemical Engineering, Soongsil University,
Sangdo-dong, Dongjak-ku,
Seoul, 156–743, Korea

C. Kim (✉)
Department of Chemical and Biological Engineering,
Korea University, Anam-dong, Sungbuk-ku,
Seoul, 136–713, Korea
e-mail: cykim@grtrkr.korea.ac.kr

Introduction

Carbon nanotubes (CNTs) have been involved diversely in biological, electronic or mechanical applications due to its mechanical and electrical properties beyond metal. The objective of CNT usage in diverse fields is to realize high-performance materials in mechanical or electrical properties with a small amount of CNT. Then, the study on the dispersion of CNTs in a matrix is critical to achieve their successful application. CNTs are not easily dispersed and it demands some dispersion steps because their aspect ratio is above 100–1,000 and therefore the nanotubes are entangled. Also, the surface area per unit mass is large and hence van der Waals force between nanotubes is strong. Even under a flow, the entangled CNT clumps are not easily disentangled. The disentanglement can be obtained only when we apply more energy against the total van der Waals force between nanotubes. The dispersion of CNTs has been studied either by hydrodynamic methods or by compatibilization methods through the modification of CNT surface (Montesi et al. 2004; Lin-Gibson et al. 2004; Potschke et al. 2004, 2008; Wu and Shaw 2006; Hobbie and Fry 2006; Start et al. 2006; Huang et al. 2006; Ma et al. 2007; Hong and Kim 2007; Pegel et al. 2008; Kang et al. 2008). Huang et al. (2006) presented that the CNT dispersion in polydimethylsiloxane was improved when CNTs stayed under the shear flow for the critical dispersion time or longer. Hong and Kim (2007) studied the CNT dispersion in polybutene under extensional flows. Under the extensional flow, the hydrodynamic friction causes tubes to unravel from entangled CNT clumps even though it still requires a long process time. In a multi-phase system, the flow to induce particle dispersion may be more

complicated because there are two additional variables of viscosity ratio and interfacial tension. But the multi-phase system can be more effective if we can properly control these variables. Now, we can seek whether the dispersion of CNTs can be improved by applying another flow pattern between immiscible phases in blends. It has been reported that the dispersion of organically modified nanoclay (organoclay) of high aspect ratio is improved in multi-phase systems by the movement of organoclay into interfacial region even though it has no chemical attraction with either phase of the blend and it resulted in the coalescence suppression effect and interfacial tension reduction effect. Also, depending on the difference in chemical affinity of organoclay with phases, it gives the selective localization and compatibilizing effect on the multi-phase system (Vermant et al. 2004; Hong et al. 2007, 2008). Organoclay has a layered structure of platelets 1 nm thick and several hundred nanometers long. The aspect ratio of each platelet is as large as 100–1,000 but the clay tactoid shows several hundred nanometers in thickness. In immiscible multi-phase systems, during morphology evolution, organoclay shows a shear-induced migration to the interface and/or to the phase that has higher chemical affinity under the given flow, which results in the coalescence suppression (Hong et al. 2008). At the same time, the breakup of the dispersed phase increased by reducing the interfacial tension by the organoclay located at the interface since the organoclay at the interface induces the Marangoni motion against shear which reduces the interfacial tension (Hong et al. 2007). If the non-homogeneous chemical potential between phases can induce CNT migration, there is a possibility that CNTs are selectively located at the phase which attracts CNTs (Baudouin et al. 2010; Bose et al. 2010) and the time to disperse CNTs can be quite reduced. Recently, Bose et al. (2010) have reported that amine-functionalized CNTs show dense localization in αMSAN/PMMA, which results in the coalescence suppression effect. Even with non-functionalized CNTs, CNTs are selectively located depending on the difference in chemical affinity in PA/EA-copolymer (Baudouin et al. 2010). Previous researches on CNT dispersion in polymer melt reported that the efficiency of CNT dispersion is improved when it is dispersed by a master batch method. However, the mechanism of the improved dispersion is still unknown.

In this study, we have investigated the behavior of CNT dispersed in PDMS/PB blend, an immiscible two-phase system. We have especially investigated the change in the blend morphology and the distribution of CNT between phases. Because CNTs are quite different from organoclay in density, surface charge and the chemical affinity with organic materials, it is difficult to predict the behavior of CNT in the multi-phase system based solely on the organoclay system. The research on the behavior of CNT in multi-phase systems is at an early stage at the moment even though industries still demand effective dispersion methods to realize better performance with CNTs such as electrical properties.

Previously, we reported the dispersion behavior of CNT in a PB solution (polyisobutylene/polybutene) under extensional flows (Hong and Kim 2007). In their case, dispersion of CNTs in the PB solution should be caused only by the hydrodynamic friction. Therefore the 0.3 wt.% CNT dispersion maintains Newtonian behavior while the viscosity increases by the contribution of hydrodynamic volume of dispersed CNTs. In this study, we have focused on the dispersion of CNTs in an immiscible two-phase system in which CNTs are subjected to different hydrodynamic friction during the process. We especially focused on the location of CNTs in a multi-component system and the modification of the immiscible PDMS/PB blend morphology by CNTs. PDMS/PB blends have been widely used in studying the morphology or rheology of immiscible solution blends (Martin and Velankar 2007; Hemelrijck et al. 2005; Tufano et al. 2008). On the other hand, the dispersion of PDMS in PB Boger fluid is rarely studied by the experimental restrictions such as the Weissenberg effect. However, when extensional flow is used, no such problems arise. The matrix of PB Boger fluid (PIB/PB) chosen in this study shows a strain hardening behavior under extensional flows (Tirtaatmadja and Sridhar 1993; Hong and Kim 2010). The increased high viscosity of PB solution under the extensional flow increases the capillary number, which effectively enhances the break-up of the dispersed domain. The study on the location of CNT in a multi-component system will give a significant hint on the successful CNT application because it can reduce the amount of CNTs required to achieve desired properties and hence the cost. Furthermore, because the PB solution used in this study has a very high viscosity (31 Pa s), this study expects to give further understanding on the CNT dispersion in the polymer melt blends.

Experimental

Materials

The immiscible solution blend chosen in the present study consists of polybutene (PB: $M_n = 920$, Sigma-Aldrich Chem. Co.) and polydimethilsiloxane (PDMS:

Table 1 Formulations of blends and blend composites and their blending conditions

Samples	Formulation			Blending condition
	wt% PDMS	wt% PB	wt% CNT	
B4	4	96	–	3 h, 0.9 s^{-1}
B12	12	88	–	extension
B20	20	80	–	
B36	36	64	–	
B4CNT008	4	95.82	0.08	3 h, 0.9 s^{-1}
B12CNT025	12	87.75	0.25	extension[a]
B20CNT025	20	79.75	0.25	
B36CNT025	36	63.75	0.25	

[a]Master batch generation condition: 1,500 s^{-1} shear, 3 h

Sylgard 184, Dow Corning Co.). The PB solution as a matrix is a blend of polybutene and a small amount (3,000 ppm) of polyisobutylene (PIB: $M_n = 3.1$ M, Sigma-Aldrich Chem. Co.) prepared by solution mixing. This PB solution, PIB/PB, is known as a Boger fluid which has a shear-independent viscosity and high elasticity (Tirtaatmadja and Sridhar 1993). It has a density of 890 kg/m^3. The density of PDMS is 1,030 kg/m^3 and its viscosity is 5.7 Pa s. The matrix, PB, has zero shear viscosity of 31 Pa s ($\approx \eta_o$) at 25°C, while, under extensional flows, the viscosity of PB matrix will be much higher than the Trouton viscosity of $3\eta_o$ due to strain hardening behavior. It can increase by as large as three orders of magnitude. For example, at the extensional rate of 0.4 s^{-1}, it is 1.3 × 10^3 Pa s and the hardening behavior is more significant as the strain rate increases (Hong and Kim 2010).

The fraction of PDMS in the PDMS/PB blend was varied from 4 to 36 wt.% as listed in Table 1. Sample IDs were given such that 4 wt.% PDMS/96 wt.% PB solution was called B4 (see Table 1 for other blends). For those blends, the master suspension of CNTs in PDMS (CNT master: the preparation of the CNT master is described below) was added as shown in Table 1. The content of CNT was fixed at 0.25 wt.% for B12, B20, and B36 which were named as B12CNT025, B20CNT025, and B36CNT025, respectively. Meanwhile, in the case of B4, the amount of CNT was reduced to 0.08% because CNT was added from the same 2 wt.% CNT master.

CNTs used in this study were multi-walled, commercial-grade nanotubes (purity > 90%, manufacturer's specification) supplied from Iljin Nanotech, Korea. It is known from the manufacturer that the CNT was prepared by a chemical vapor deposition method by the reaction of a carbon-containing gas such as acetylene, ethylene, ethanol, etc. with a metal catalyst at above 600°C. The diameter and the length of a single tube are in the range of 10–20 nm and 10–50 μm, respectively, according to the manufacturer's specification. CNTs of high aspect ratio form the entangled tube clumps. Each clump is a heterogeneous particle of a broad-size distribution from a few to several hundred micrometers.

Blending

In this study, the preparation of CNT dispersions was accomplished in two steps as shown in Fig. 1. The first step is the generation of CNT master and the second

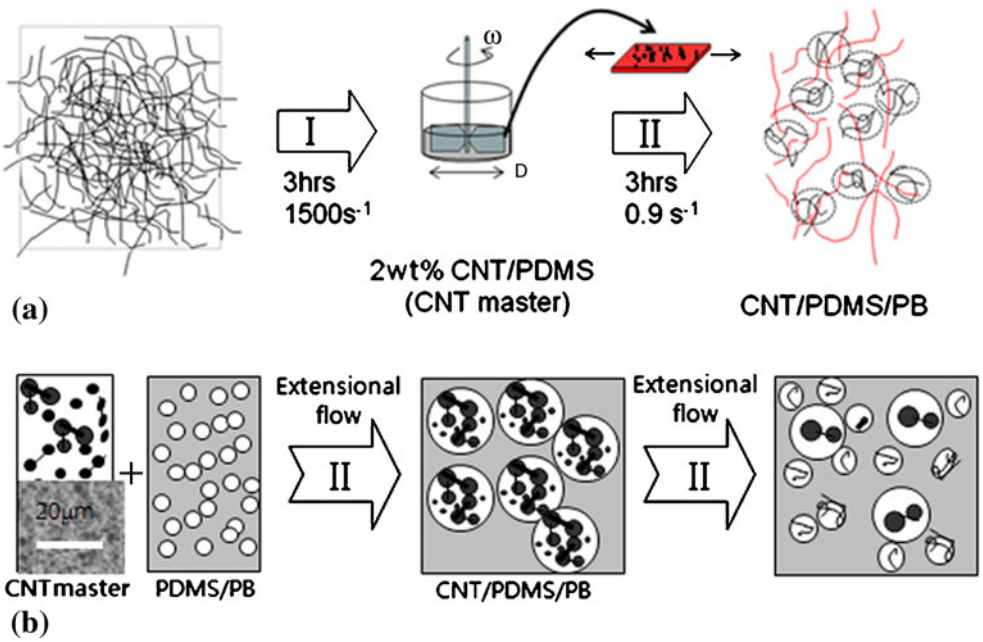

Fig. 1 Schematic diagram of the dispersion of CNTs. **a** Two-step dispersion method: *step I*, CNT master (2 wt.% CNT/PDMS) is prepared by mechanical stirrer ($\dot{\gamma}$ = 1,500 s^{-1}, 3 h); *step II*, the CNT master is diluted under an extensional flow (0.9 s^{-1}, 3 h). **b** In *step II*, a small amount of CNT master is added during the blending of PDMS and PB

step is the dilution of the CNT master to the matrix (PB) or PDMS/PB blend. It has been well known that CNT master batch dilution method effectively improves the dispersion of CNT in polymer melt such as PC or PA (Pegel et al. 2008; Potschke et al. 2004). For the CNT master, two parts of CNT powders were mixed with 98 parts of PDMS by using a mechanical stirrer in a beaker for 3 h. The diameter of the rotor (D) was 60 mm and the gap distance between the rotor tip and the beaker wall (H) was 1.5 mm. The rotor speed was 700 rpm so that the apparent shear rate was 1,500 s^{-1}. The CNT master was diluted to the PDMS/PB blend for 3 h using the same "extension-induced mixer" as used in the dispersion of CNTs in viscoelastic fluid (Hong and Kim 2007). In the extensional mixer, the extensional deformation was continuously applied to the blend by stretching and folding the sample repeatedly by the rotations of two axes. The whole process can be characterized by an apparent extensional rate which is proportional to the rotational rate of the arms.

In this research, the extension was performed at the apparent extensional rate ($\dot{\varepsilon}$) of 0.9 s^{-1} for 3 h. Again, for the dispersion of CNT in the PDMS/PB blend, a desired amount of CNT master was added to the PDMS/PB blend in the same manner. Each blend listed in Table 1 (B4, B12, B20, and B36) was prepared at the same extensional condition.

Characterization

Rheological properties of the blends and CNT dispersion were measured by using a controlled-strain rheometer (AR2000, TA instruments). The complex viscosity and storage modulus were measured in the dynamic mode with a parallel plate fixture (30 mm diameter). The morphology was examined under an optical microscope (BX-51, Olympus) and a cryo-TEM (JEM 2100F, JEOL Ltd.). To analyze the morphology quantitatively, the number averaged domain size was obtained with an image analyzing software (Image-Pro, Media Cybernetics Inc.). The number-averaged drop size was determined from the arithmetic mean of drop diameter (D_i) for N-drops ($D_n = \Sigma D_i / N$). Here, we have included only the drops that can be identified under the optical microscope.

Results and discussion

In the present study, the rheology and morphology of CNT-dispersed PDMS/PB blends have been investigated to understand the effect of CNTs dispersed in the PDMS/PB blend. To understand the effect of CNTs, we first prepared the samples without dispersing CNTs and investigated their rheological and morphological characteristics. Figure 2 shows the morphology of samples

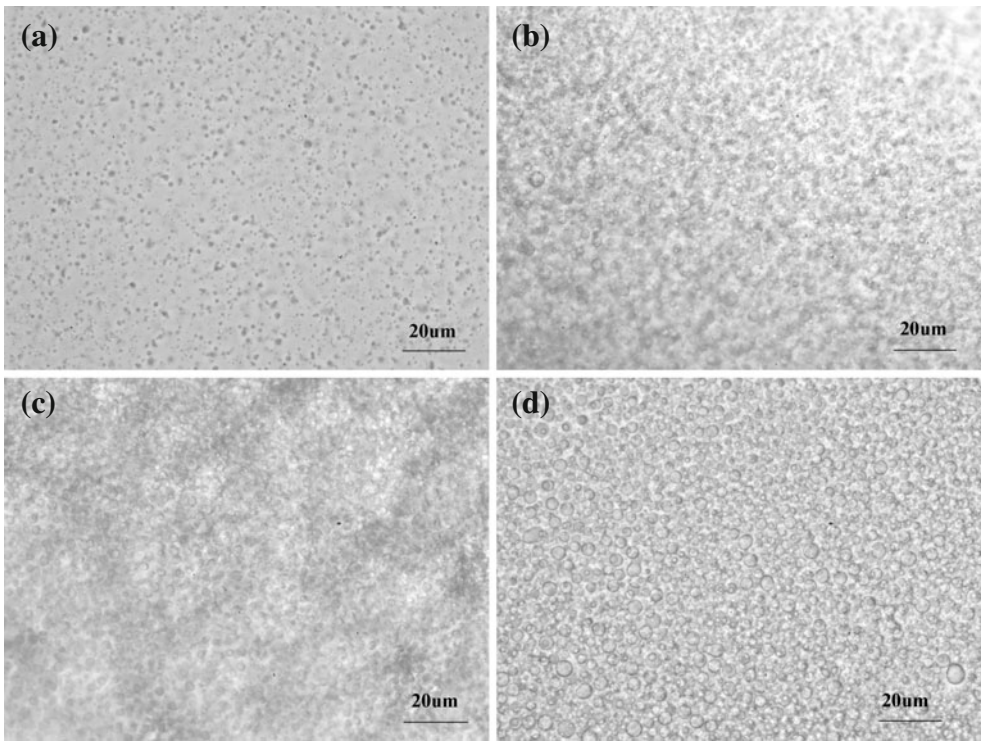

Fig. 2 Microscopic pictures of PDMS/PB blends: B4 (**a**), B12 (**b**), B20 (**c**), and B36 (**d**)

B4, B12, B20 and B36 examined under an optical microscope using the objective lens of a magnification of 40×. Here, up to 36% of PDMS (B36), the PDMS drop sizes are small and the drop size distributions are quite uniform. The smallness and uniformity of drop size are the characteristics of the extensional mixer (Hong and Kim 2010): when using the mixer PDMS drops are broken up by the highly increased viscosity of PB solution due to strain hardening, which effectively enhances the break-up of the dispersed domain to result in the small drop size through the increase in capillary number. At the same time, the coalescence effect between drops which is expected when the fraction of the dispersed phase increases rarely occurs under extensional flows to result in the uniformity in drop size. Therefore, the average drop size of PDMS is not much changed over a wide range of PDMS content. Even B36 shows the droplet size of 4.0 μm, which may not be possible with a conventional shear mixing method. In this study, the capillary number ($\mathrm{Ca} = \eta_{\mathrm{medium}}\dot{\varepsilon}\mathrm{D}/\Gamma$) at the blending condition was chosen so that it is larger than the critical Ca ($\mathrm{Ca_{cr}}$) of $0.148(\eta_{\mathrm{medium}}/\eta_{\mathrm{drop}})^{1/6}$ (Acrivos and Lo 1978). In the present experiment, the drop size is 4 μm, the strain-hardened viscosity of PB phase is above 600 Pa s ($\eta_{\mathrm{eo}} \approx 3\eta_{\mathrm{o}} = 30$ Pa s and $\eta_{\mathrm{e}}^{+}/\eta_{\mathrm{eo}} > 20$ at 0.4 $\mathrm{s^{-1}}$; Hong and Kim 2010), the extension rate is 0.9 $\mathrm{s^{-1}}$ and the interfacial tension is approximately 2 mN/m (Tufano et al. 2008). Then Ca is 1.1, which is much larger than $\mathrm{Ca_{cr}}$ for extensional flows of 0.3 at the given viscosity ratio. Under this condition, the increased hydrodynamic stress due to strain hardening leads the break-up of the dispersed phase. Because the average drop size does not change much, it is expected that the total interfacial force is effectively increased as PDMS fraction increases, which should affect the rheological property.

In Fig. 3, η^* and G' of the blends are compared. As expected, both η^* and G' of PDMS/PB increase with the increase in the amount of PDMS even though the viscosity of PDMS is much lower than the viscosity of PB. It is caused by the dominant contribution of large interfacial area. The total interfacial area of blend is significantly increased with the fraction of PDMS because the drop size does not change with the concentration of PDMS. The storage modulus (G') of blend is known to be increased by the increased contribution of interfacial area as follows (Larson 1999):

$$G'_{\mathrm{blend}} = \phi_{\mathrm{PB}}G'_{\mathrm{PB}} + \phi_{\mathrm{PDMS}}G'_{\mathrm{PDMS}} + G'_{\mathrm{interface}} \quad (1)$$

where ϕ is volume fraction. If the contributions from PB and PDMS are linearly added ($= \phi_{\mathrm{PB}}G'_{\mathrm{PB}} + \phi_{\mathrm{PDMS}}G'_{\mathrm{PDMS}}$), G'_{blend} will become smaller as PDMS fraction increases due to the lower value of G'_{PDMS} than G'_{PB}. It means that the increase in storage modulus of blend especially at the low frequency region ($\leq$10 $\mathrm{s^{-1}}$) is caused by the significant contribution of the interfacial tension, $G'_{\mathrm{interface}}$. At the low frequency region of 0.1 through 10 $\mathrm{s^{-1}}$, Ca ($= \eta_{\mathrm{medium}}\dot{\gamma}\mathrm{D}/\Gamma$) varies from 0.0062 to 0.62. This range of Ca is much lower than $\mathrm{Ca_{cr}}$ for shear flows of 1.0 (Taylor 1934). It means that the interfacial tension resists against the drop deformation at the low frequency range. This resistance is reflected on the increase in G' and η^* with PDMS content.

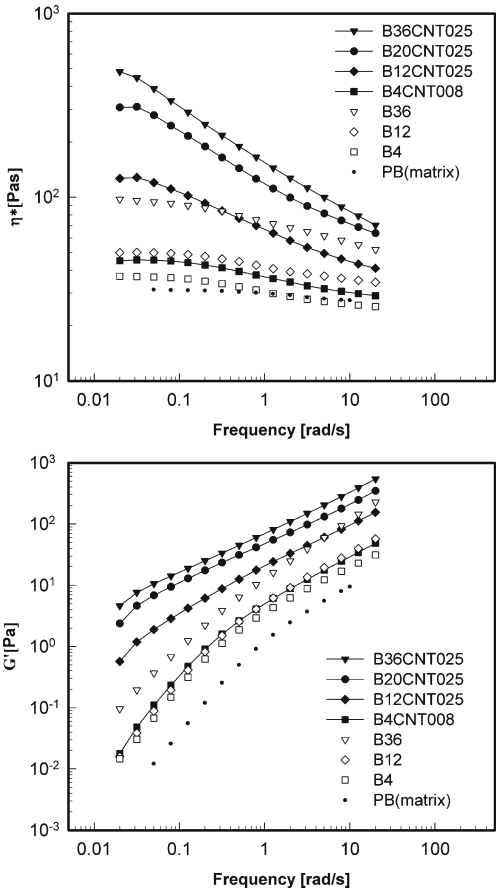

Fig. 3 Rheological properties of blends and CNT blend dispersions: complex viscosity (**a**) and storage modulus (**b**)

Next, we consider the CNT dispersed blends. Based on rheological and morphological observations, the PB/PDMS blends do not show any miscibility for the range of compositions considered here. If CNTs with such a high aspect ratio are dispersed in an immiscible PB/PDMS blend, the rheological properties of blend are strongly dependent on the location of CNTs. If CNTs are still located inside the dispersed phase, the increase in viscosity is hardly expected because the viscosity of the dispersed phase is not much affecting

the viscosity of the blend as described above. On the other hand, if CNTs are dispersed and located at the interface or at the matrix and if they are close enough to interact hydrodynamically, the rheological properties of composite such as viscosity or G' may change significantly. In the present study, even with a small amount of CNTs in PB/PDMS blend (0.08–0.25 wt.%), the viscosity increases significantly as shown in Fig. 3 and Table 2. Therefore, it is difficult to say that CNTs stay within the dispersed phase of blend. However, the change in rheological properties alone cannot tell the reason for the increase in rheological properties. The reason for the increase will be considered later when the morphology of the blend is considered.

The equilibrium distribution of CNT particles between PDMS and PB phases can be predicted by a theory based on the wetting coefficient analysis of Young's equation (Wu 1982):

$$\omega = \left(\gamma_{\mathrm{CNT/PDMS}} - \gamma_{\mathrm{CNT/PB}}\right)/\gamma_{\mathrm{PB/PDMS}} \tag{2}$$

If the wetting coefficient, ω is higher than 1 CNT goes to the PB phase, while if it is less than −1 CNT is preferentially located in the PDMS phase. Here, interfacial energy $\gamma_{A/B}$ is calculated by the following expression (Wu 1982):

$$\gamma_{A/B} = \gamma_A + \gamma_B - 4\left(\gamma_A^d\gamma_B^d/\left(\gamma_A^d + \gamma_B^d\right) + \gamma_A^p\gamma_B^p/\left(\gamma_A^p + \gamma_B^p\right)\right) \tag{3}$$

If numerical data listed in Table 3 are used it is found that $\gamma_{\mathrm{CNT/PDMS}} \sim 8.09$ m Jm^{-2}, $\gamma_{\mathrm{CNT/PB}} \sim 15.2$ m Jm^{-2}, $\gamma_{\mathrm{PB/PDMS}} \sim 4.85$ m Jm^{-2} and ω of the system is −1.46. Therefore, CNT will be preferentially located in PDMS rather than in PB.

In this research, the content of CNT is fixed at 0.25 wt.% for the samples that contain 12–36 wt.% of PDMS in PDMS/PB blends, while the content of CNT is 0.08 wt.% for the sample that contains 4 wt.% PDMS. The CNT dispersed blend is renamed, for example, as B12CNT025 for the sample containing 12% PDMS in the blend together with 0.25 wt.% of CNTs. Figure 4 shows the morphologies of these CNT dispersed PDMS/PB blends following mixing. In the case of B4CNT008, the size of PDMS drop is not changed much with the addition of CNTs. First, we note that CNT particles are observed as blurred images. This is because CNT particles are not easily focused with the 40× objective lens meaning that the particles are larger than the depth of field of the lens (1.0 μm for 40× objective lens). In Fig. 4d, most of the CNTs appear to be located at the interface of PDMS and PB, as in the case of organoclay, in blends (Hong et al. 2007). Also, some CNTs are observed out of the PDMS phase. For B12CNT025, CNTs are still observed out of PDMS phase. When PDMS fraction is increased to 20 wt.% (B20CNT025), the drop size of PDMS is much larger than that of B20 and the size distribution becomes broader. Especially for B36CNT025, some CNT particles are observed both inside and outside of PDMS drops. Later, we will show that, by cryo-TEM analysis, CNTs are not actually located at the interface. Rather, many small drops containing a single CNT are generated by the extensional flow and these small drops remain around the large mother drop of PDMS. Since these small drops cannot be resolved under the optical microscope, the small drops that contain CNTs appear to be located within the matrix phase or at the interface even though they are enclosed by a very small PDMS drops. Therefore, the present experimental result does not violate the thermodynamic preference in the location of CNTs as discussed above. Figure 5 compares the average drop size of PDMS/PB blends and CNT-dispersed PDMS/PB blends. The average PDMS drop size increases with the addition of CNT and the size distribution becomes broader with the concentration of PDMS. Especially in the case of B36CNT025, the average PDMS drop size increases from 4 (for B36) to 11 μm and the distribution becomes

Table 2 Storage modulus of blends and CNT dispersion

Materials	G'_{measured} at 0.05 s^{-1} (Pa)	$\Sigma\phi_i G'_i$ at 0.05 s^{-1} (Pa)	$G'_{\mathrm{interface}}$ [a]	Effect of CNT[b]
CNT master	450	–	–	–
Matrix	0.012	–	–	–
B4	0.067	0.012	0.056	–
B12	0.09	0.011	0.079	–
B36	0.4	0.008	0.39	–
B4CNT008	0.09	14	(≤0.056)	0.023
B12CNT025	1.9	≈43	(≤0.079)	1.0
B36CNT025	10.6	≈43	(≤0.39)	10.2
B0CNT025	0.3	≈43	–	0.3

[a] $G'_{\mathrm{measured}} - \Sigma\phi_i G'_i$

[b] $G'_{\mathrm{blend\ measured}} - G'_{\mathrm{CNT/blend\ measured}}$

Table 3 Surface energy of materials

Materials	Total surface energy (γ) m Jm^{-2}	Dispersive surface energy (γ^d) m Jm^{-2}	Polar surface energy (γ^p) m Jm^{-2}
CNT[a]	27.8	17.6	10.2
PDMS[b]	19.8	19.0	0.8
PB[b]	33.6	33.6	0

[a] Source: Baudouin et al. (2010)

[b] Source: http://www.surface-tension.de/solid-surface-energy.htm

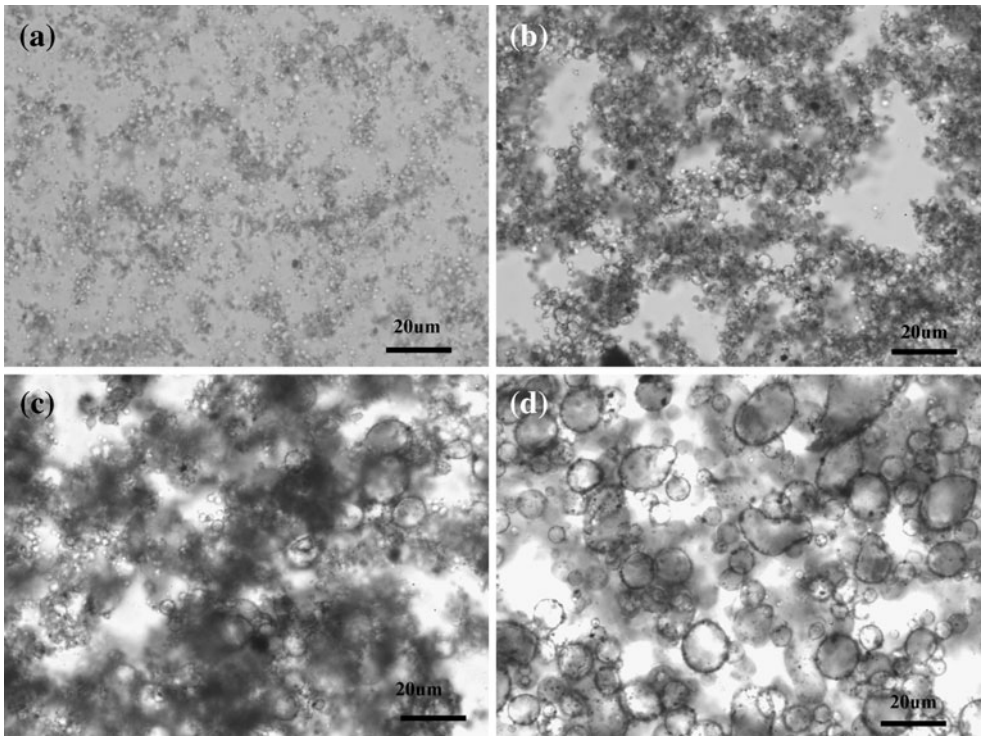

Fig. 4 Microscopic pictures of CNT blend dispersions: B4CNT008 (**a**), B12CNT025 (**b**), B20CNT025 (**c**), and B36CNT025 (**d**)

significantly broader. Compared with the blend without CNTs, the increase in drop size with CNTs should be caused by the high viscosity of the CNT master ($D_{avg} = 0.148\Gamma(\eta_{medium}/\eta_{drop})^{\alpha}/\eta_{medium}\dot{\varepsilon}$, here $\alpha > 0$ for $p < 1$ and $\alpha < 0$ for $p > 1$, $p = \eta_{drop}/\eta_{medium}$, $|\alpha| = 1/6$; Acrivos and Lo 1978). The extensional viscosity ratio (p) increases from 0.03 to 50 with CNT (17 Pa s for PDMS ($\approx 3 \times 5.7$ Pa s), 600 Pa s for PB, 30,000 for CNT master ($\approx 3 \times 10{,}000$ Pa s), approximately), which changes the morphology evolution of blend because the change in p results in the change in Ca_{cr} which determines the drop size. The difference among the drop sizes of B12CNT025 through B36CNT025 appears to be caused by the distribution of CNTs which affects the viscosity ratio. It appears that the difference in drop size among samples with differing PDMS content is dependent on the amount of CNT containing PDMS drops which are taken off from the mother drop. Wherever CNTs are located, the drop size of the blend containing CNTs seems to increase with PDMS fraction.

Another important factor in morphology evolution is interfacial tension. In blend nanocomposites, organoclay particles are located at the interface during the morphology evolution and it results in the change of interfacial tension as well as morphology. For example, the number averaged drop size reduces to 1 μm from 3 μm for a HDPE/PBT blend containing 3 wt.% organoclay (Hong et al. 2007). Meanwhile, CNTs do not seem to have any compatibilizing effect such as reduction in drop size between immiscible components like organoclay.

To investigate the compatibilization effect of CNTs, it is necessary to examine where CNTs are located in immiscible blends. Figure 6 shows the cryo-TEM observations of the CNT master (Fig. 6a) and B12CNT025 (Fig. 6b and c). In the case of the CNT, master CNTs

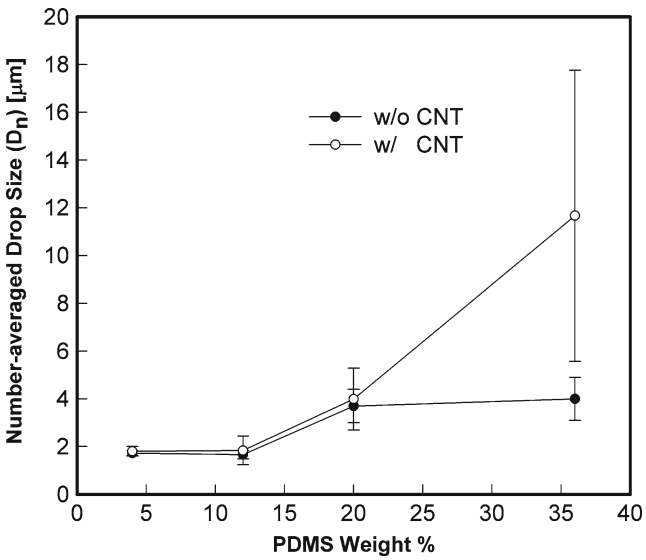

Fig. 5 Comparison of the number averaged-drop size of blends and CNT blend dispersions

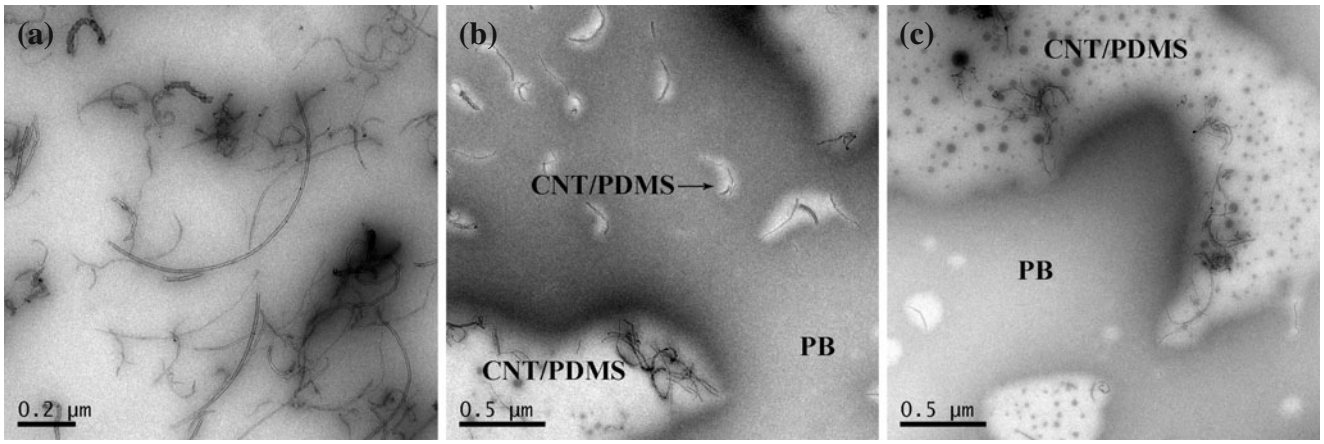

Fig. 6 Cryo-TEM images of CNT master (**a**) and B12CNT025 (**b**, **c**)

are hydrodynamically close enough to build a rheological percolation, from which we can confirm that viscosity and storage modulus should increase with the addition of CNTs. We note that the CNTs have shorter lengths than the manufacturer's specification. It appears that most of the tubes were broken during the preparation of the master batch. In CNT dispersed blends (Fig. 6b and c), some densely entangled tubes like a thread kink are still observed but its scale is obviously reduced to sub-micrometers. Especially some small drops including unraveled CNTs are frequently observed. These TEM images show that there exist many small PDMS drops and many of them contain single CNT. Even though CNTs appear to be located both inside and outside of PDMS phase in Fig. 4, the TEM images show that this is not the case. This is due to the inherent problem of low resolving power of the optical microscope. It is also observed that the CNT concentration in the CNT master phase is lowered. Some of the CNTs in the original CNT master phase appear to move out of the CNT master phase. The existence of small drops containing CNTs means that under the extensional flow, small drops including CNTs are broken up from mother drops during morphology evolution. This dispersion behavior reduces the dispersion time needed when CNTs are dispersed only by hydrodynamic friction in a continuum due to the reason as follows: If a single CNT is assumed to be a long fiber ($L/d > 20$), CNTs cannot migrate during the observation time scale of less than 10,000 s due to the high viscosity of matrix (η_s) if we consider the small diffusivity of long fibers. The translational diffusion constant ($D_{||}$) for rods is known to have the relation of $D_{||} = L^2 D_{ro}$ if perpendicular motions are neglected. The rotational diffusion coefficient $D_{ro} = 3\ k_B T(\ln(2L/d) - 0.5)/\pi\eta_s L^3$ has $\sim O(10^{-5}\ \mathrm{m^2\ s^{-1}})$ for $L/d = 20$, $L = 1$ μm and $\eta_s = 1{,}000$ Pa s (Doi and Edwards 1986) and hence $D_{||}$ has $\sim O(10^{-17}\ \mathrm{m^2\ s^{-1}})$. Therefore, it is certain that CNTs are difficult to migrate to the other phase in such a short time even for the case of unraveled CNTs from entangled CNT clumps. Therefore, the non-Brownian CNTs can be dispersed only by flows ($\mathrm{Pe} = \dot{\varepsilon}/D \sim 10^{16} >> 1$ at $\dot{\varepsilon} = 0.9\ \mathrm{s^{-1}}$). Under the extensional flow, the morphology evolution

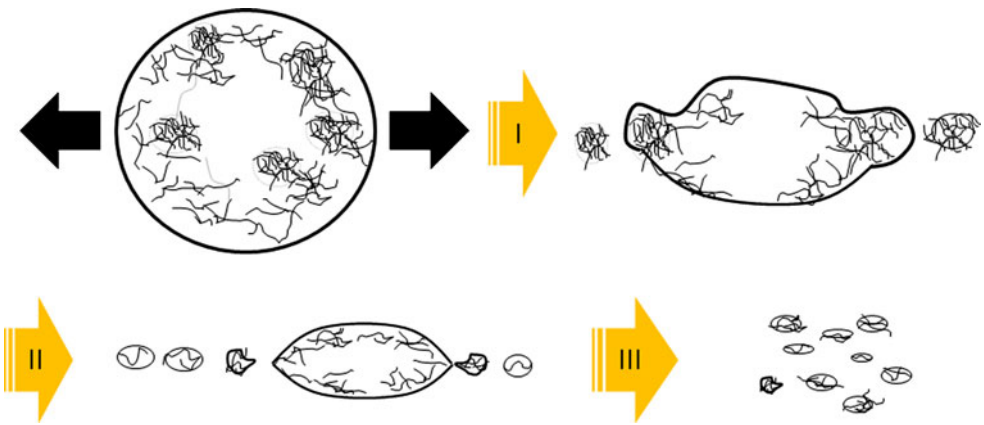

Fig. 7 Dispersion of CNTs in PDMS/PB blends by the pinching off mechanism

simultaneously occurs with the flow induced-migration of CNT. However, it appears that the morphology evolution dominantly leads the CNT dispersion since the flow induced migration of CNT requires long time. Under the extensional flow, CNT master phases are dominantly broken up by tip-streaming because the viscosity ratio is much higher than 10 (Miliken and Leal 1991). As shown at Fig. 7, the tip-streaming results in the dispersion of individual tubes without being placed at the interface. Based on the morphology observations, we can infer that small drops including single tubes are pinched off from the CNT master phase under the extensional flow and CNTs are not located at the interface.

Rheological observations also support the pinching-off of small drops with CNTs from the dispersed phase. The rheological properties of CNT dispersed blends should be determined by the contribution from each component of the blend, CNT master and the interface. Then, the storage modulus of the CNT dispersed blend can be written as follows:

$$G'_{\text{blend-dispersion}} = \phi_{\text{PB}} G'_{\text{PB}} + \phi_{\text{PDMS}} G'_{\text{PDMS}} + \phi_{\text{CNTmaster}} G'_{\text{CNTmaster}} + G'_{\text{interface}}. \quad (4)$$

This rule is supposed to be valid when the percolation structure of CNT master persists after mixing. When this formula is applied to the sample B4CNT008 (4% CNT, $G'_{\text{CNTmaster}} = 450$ Pa), $G'_{\text{blend-dispersion}} = 18$ Pa + $G'_{\text{interface}}$. However the measured G' of 0.09 Pa is much lower than this expectation as shown in Table 2. Other samples show similar results as listed in Table 2. This is in contrast with the fact that G'_{blend} values of B4, B12 and B36 are positively deviated from the linear mixing rule, $G'_{\text{blend}} = \Sigma \phi_{\text{i}} G'_{\text{i}}$. The deviation of $G'_{\text{blend-dispersion}}$ from the mixing rule implies that CNTs should be moved from the CNT master phase to the matrix phase in some ways (actually by tip-streaming as the TEM images show), which changes the CNT concentration of the CNT master as the previous observation on morphological characteristics shows. The dispersion of CNTs out of the CNT master phase means that G' of the CNT master should be lowered since the concentration of CNT is reduced and the percolation structure of the CNT master is lost. Then, $G'_{\text{CNTmaster}}$ no longer follows the mixing rule (Eq. 2) and can be decreased as the blend morphology changes further. On the other hand, the contribution of interfacial tension on rheological properties may not be simply reduced even though it is expected to decrease with the increase in the drop size with the addition of CNTs. Here, we cannot determine $G'_{\text{interface}}$ for CNT dispersed samples by measuring the G' values of each component and the CNT dispersed samples since the mixing rule does not apply to this system due to the fundamental change in morphology. In reality, many submicron-sized drops are found with CNTs, which should contribute to the increase in the rheological property of matrix while the CNT density in the CNT master is diluted. The filling effect of CNT on the matrix becomes more significant as the content of PDMS increases from 12% to 36%. Then, the rheological properties increase as the fraction of PDMS increases while the CNT content is fixed. This is already shown in Fig. 3 where η^* of B36CNT025 is far larger than η^* of B12CNT025. The rheological observations give consistent results with the previous morphological observations that CNTs are moved from the CNT master phase to the matrix phase under the extensional flow without interface modification.

Conclusion

In this study, CNTs are dispersed in immiscible PDMS/PB blends by a two-step dilution method. At the first step, the CNT master is prepared by the conventional stirring method. At the second step, the CNT master is mixed with the PDMS/PB blend under an extensional flow. During the morphology evolution under the extensional flow, the CNT master phase is broken up by tip-streaming and small PDMS drops including CNTs are pinched-off due to the high viscosity ratio. This results in a non-homogeneous size distribution. CNTs are not found to be located at the interface. The pinching-off of CNTs from the CNT master phase reduces the concentration of the CNT inside master and, at the same time the dispersed CNT containing droplets are dispersed in the matrix. The filling effect of CNTs to the matrix is more significant as the content of PDMS increases. The pinching-off of small drops during morphology evolution improves the CNT dispersion as a consequence.

In this study, by using the two-step dilution method and extensional mixing process, we have shown that CNTs can be disentangled as in the case of dispersing CNTs in a single-phase liquid such as Boger fluid. In this case, tip streaming is one of the major mechanisms for the dispersion. Rheological data and TEM observations show that it is not simply a mixing of two phases and the CNTs in the master phase can be dispersed in the single CNT level. This study can shed light on further understanding of CNT dispersion in various kinds of liquids including polymer melts.

Acknowledgements This work was supported by Mid-career Researcher Program through NRF grant funded by the MEST, Korea (No. 2010-0015186).

References

Acrivos A, Lo TS (1978) Deformation and breakup of a single slender drop in an extensional flow. J Fluid Mech 86:641–672

Baudouin AC, Devaux J, Bailly C (2010) Localization of carbon nanotubes at the interface in blends of polyamide and ethylene–acrylate copolymer. Polymer 51:1341–1354

Bose S, Ozdilek C, Leys J, Sew JW, Wubbenhorst M, Vermant J, Moldenaers P (2010) Phase separation as a tool to control dispersion of multiwall carbon nanotubes in polymeric blends. App Mat Interfaces 2(3):800–807

Doi M, Edwards SF (1986) The theory of polymer dynamics. Oxford University Press, New York

Hemelrijck EV, Puyvelde PV, Macosko CW, Moldenaers P (2005) The effect of block copolymer architecture on the coalescence and interfacial elasticity in compatibilized polymer blends. J Rheol 49(3):783–798

Hobbie EK, Fry DJ (2006) Nonequilibrium phase diagram of sticky nanotube suspensions. Phys Rev Lett 97:036101

Hong JS, Kim C (2007) Extension-induced dispersion of multiwalled carbon nanotube in non-Newtonian fluid. J Rheol 51:833–850

Hong JS, Kim C (2010) Generation of sub-micron-sized droplets, by continuous extensional flow. J Non-Newt Fluid Mech 165: 681–686

Hong JS, Kim YK, Ahn KH, Lee SJ, Kim C (2007) Interfacial tension reduction of PBT/PE blends by nanoclay. Rheol Acta 46(4):469–478

Hong JS, Kim YK, Ahn KH, Lee SJ (2008) Shear-induced migration of nanoclay during morphology evolution of PBT/PS blend. J App Polym Sci 108:565–575

Huang YY, Ahir SV, Terentjev EM (2006) Dispersion rheology of carbon nanotubes in a polymer matrix. Phys Rev B 73: 125422

Kang J, Lee J, Kim TH, Park J, Seong MJ, Hong S (2008) Large scale assembly of carbon Nanotube based flexible circuits for DNA sensors. Nanotechnology 19:135305

Larson RG (1999) The structure and rheology of complex fluids. Oxford University Press, New York

Lin-Gibson S, Pathak JA, Grulke EA, Wang H, Hobbie EK (2004) Elastic flow instability in nanotube suspensions. Phys Rev Lett 92(4):048302

Ma AWK, Mackley MR, Rahatekar SS (2007) Experimental observation on the flow-induced assembly of carbon nanotube suspensions to form helical bands. Rheol Acta 46:979–987

Martin JD, Velankar SS (2007) Effect of compatibilizer on immiscible polymer blends near phase inversion. J Rheol 51(4): 669–6992

Miliken WJ, Leal LG (1991) Deformation and breakup of viscoelastic drops in planar extensional flows. J Non-Newt Fluid Mech 40:355–379

Montesi A, Pena AA, Pasquali M (2004) Volticity alignment and negative normal stresses in sheared attractive emulsions. Phys Rev Lett 92(5):058303

Pegel S, Potschke P, Petzold G, Alig I, Dudkin SM, Lellinger D (2008) Dispersion, agglomeration, and network formation of multiwalled carbon nanotubes in polycarbonate melts. Polymer 49:974–984

Potschke P, Bhattacharyya AR, Janke A (2004) Melt mixing of polycarbonate with multiwalled carbon nanotubes: microscopic studies on the state of dispersion. Eur Polym J 40: 137–148

Potschke P, Pegel S, Clases M, Bonduel D (2008) A novel strategy to incorporate carbon nanotubes into thermoplastic matrices. Macro Rapid Comm 29:244–251

Start PR, Hudson SD, Hobbie EK, Migler KB (2006) Breakup of carbon nanotube flocs in microfluidic traps. J Colloid Int Sci 297:631–636

Taylor GI (1934) The formation of emulsions in definable fields of flow. Proc R Soc London Ser A 146:501–523

Tirtaatmadja V, Sridhar T (1993) A filament stretching device for measurement of extensional viscosity. J Rheol 37:1081–1102

Tufano C, Peters GW, Meijer HEH (2008) Confined flow of polymer blends. Langmuir 24(9):4494–4505

Vermant J, Cioccolo G, Nair K G and Moldenaers P (2004) Coalescence suppression in model immiscible polymer blends by nano-sized colloidal particles. Rheol Acta 43(5): 529–538

Wu S (1982) Polymer interface and adhesion. Marcel Dekker, New York

Wu M, Shaw L (2006) Electrical and mechanical behaviors of carbon nanotube filled polymer blends. J App Polym Sci 99:477–488